

Simulation of Medium-Frequency R-Mode Signal Strength

Jaewon Yu

School of Integrated Technology
Yonsei University
Incheon, Republic of Korea
jaewon.yu@yonsei.ac.kr

Joon Hyo Rhee*

Korea Research Institute of Standards and Science
Daejeon, Republic of Korea
jh.rhee@kriss.re.kr
* Corresponding author

Abstract—Assuming failure in the global navigation satellite systems due to radio frequency interference and ionospheric anomaly, an R-Mode system, a terrestrial integrated navigation system, is being actively studied for domestic deployment in South Korea. In this study, parameters for an approximate calculation of the received signal strength were obtained and applied to develop a performance simulation tool for a medium-frequency R-Mode system. As a case study, the signal strength from the Yeongju transmitter was simulated using the proposed parameters.

Index Terms—medium-frequency (MF) R-Mode system, signal strength simulation, terrestrial navigation system

I. INTRODUCTION

The global navigation satellite systems (GNSS), including the GPS [1] of the U.S. and Galileo of Europe, are widely used to obtain the locations of users based on the received signals from satellites. However, GNSS is susceptible to radio frequency interference [2]–[6] and ionospheric anomaly [7]–[13]. GNSS interference cases have been reported worldwide, and South Korea has been subjected to North Korea’s intentional GPS jamming on multiple occasions since 2010 [14], [15].

South Korea is developing an R-Mode system, a terrestrial integrated navigation system, as one of the backup navigation systems for ships if the GNSS fails [16]–[18]. There are numerous studies regarding positioning and navigation under GNSS outages [19]–[34]. R-Mode utilizes the existing radio signals of opportunity for obtaining position, navigation, and time (PNT) information. Compared with eLoran [35]–[41], R-Mode can provide PNT at a relatively lower investment cost for a new radio navigation infrastructure [42]–[47]. Unlike the eLoran system, R-Mode utilizes a medium-frequency (MF) differential GNSS (DGNSS) signal or a very high frequency (VHF) automatic identification system (AIS) signal [44]–[46].

To build an R-Mode system in Korea, a simulation tool that predicts the positioning performance of the system is useful. The simulation tool that we are developing will calculate the signal strength and noise value at a given location and predict the positioning performance of the system based on the calculated signal-to-noise ratio (SNR) value. Simulation tools for predicting eLoran performance have been developed [48], [49]; however, a simulation tool for predicting MF or

VHF R-Mode performance requires further development [50]. In this study, parameters for an approximate calculation of the received signal strength were obtained and applied to develop a performance simulation tool for an MF R-Mode system.

II. METHODOLOGY

A. Approximate signal strength calculation

Lo *et al.* [49] utilized (1) to calculate the eLoran received signal strength at a given location. There are other formulas with better accuracy but they require extensive computation time. Thus, (1) is useful approximation for fast computation with reasonable accuracy.

$$\begin{aligned} \text{signal strength [dB}(\mu\text{V/m)}] \\ = 189.353 - 10 \log r^2 - \sum_i ea_i r_i \end{aligned} \quad (1)$$

Here, ea_i denotes the extra signal attenuation per unit distance at grid i , r_i denotes the signal travel distance in meters within grid i , and r denotes the signal travel distance from a transmitter to a receiver in meters. Thus, $ea_i r_i$ is the extra attenuation at grid i , and $\sum_i ea_i r_i$ is the total extra attenuation along the signal propagation path from a transmitter to a receiver. This is called *extra attenuation* because it is additional signal attenuation to the r^2 attenuation. This extra attenuation is mainly affected by the ground conductivity along the propagation path.

The ea_i can be obtained based on the results from GRWAVE [51]. GRWAVE calculates signal strength according to the given ground conductivity and center frequency, which was used in the previous eLoran simulator study [48]. Although the results from GRWAVE are reliable, the approximate formula in (1) provides significantly faster results. Fast computation is important when we need to calculate the signal strengths at numerous grid points over Korea.

B. MF R-Mode signal strength calculation

We use the same idea with (1) of the eLoran case; however, a constant C and an exponent e need to be determined in

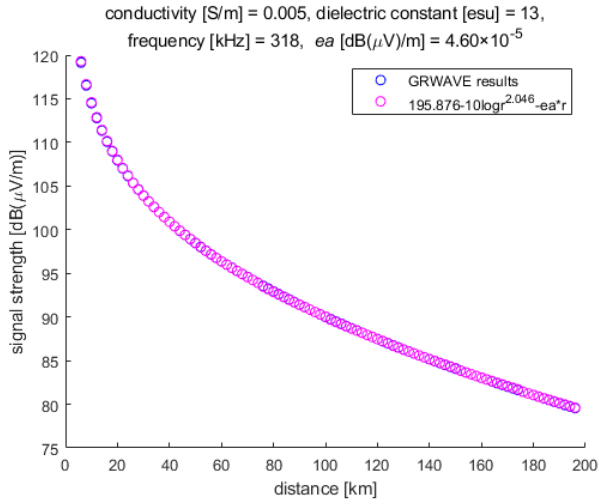


Fig. 1. Comparison of MF R-Mode signal strength simulation results from GRWAVE and our approximate formula when the ground conductivity is 0.005 S/m.

addition to ea_i for MF R-Mode signal strength calculation as shown in (2).

$$\begin{aligned} \text{signal strength [dB}(\mu\text{V/m)}] \\ = C - 10 \log r^e - \sum_i ea_i r_i \end{aligned} \quad (2)$$

The C and e are fixed values but ea_i depends on the ground conductivity. When the ground conductivity is 0.005 S/m, for example, GRWAVE provides the signal strength according to the propagation distance, which is shown as the blue circles in Fig. 1. The pink circles represent the signal strength from the approximate formula of (3), which is the special case of (2) when the ground conductivity is constant over all grids.

$$\begin{aligned} \text{signal strength [dB}(\mu\text{V/m)}] \\ = C - 10 \log r^e - ea \cdot r \end{aligned} \quad (3)$$

The pink circles in Fig. 1 are almost identical to the blue circles when ea is 4.60×10^{-5} dB(μ V/m). This ea value was obtained by curve fitting in the least squares sense.

The C and e values of (2) and (3) were also obtained by curve fitting. $C = 195.876$ and $e = 2.046$ provide the minimum least squares error over all the ground conductivity cases of Table I. The ea values that we obtained for various ground conductivity values are summarized in Table I.

III. RESULTS AND DISCUSSIONS

The result of MF R-Mode signal strength simulation over Korea with the parameters of Table I is presented in Fig. 2 when the transmitter is in Yeongju. The actual coordinates of the current Korean MF R-Mode testbed transmitter in Yeongju were used. As proposed in [48], a land cover map was used to determine the ground conductivity of the Korean region.

Considering the different ea values for different ground conductivity listed in Table I, the signal strength of the MF R-Mode system significantly varies depending on the

TABLE I
EXTRA ATTENUATION PER UNIT DISTANCE ACCORDING TO THE GROUND CONDUCTIVITY WHEN $C=195.876$ AND $e=2.046$

| conductivity [S/m] | ea for MF R-Mode signal [dB(μ V/m)] |
|--------------------|--|
| 5×10^{-4} | 2.24×10^{-4} |
| 1×10^{-3} | 1.64×10^{-4} |
| 2×10^{-3} | 1.04×10^{-4} |
| 5×10^{-3} | 4.60×10^{-5} |
| 8×10^{-3} | 2.89×10^{-5} |
| 1×10^{-2} | 2.37×10^{-5} |
| 4 | -5.40×10^{-7} |

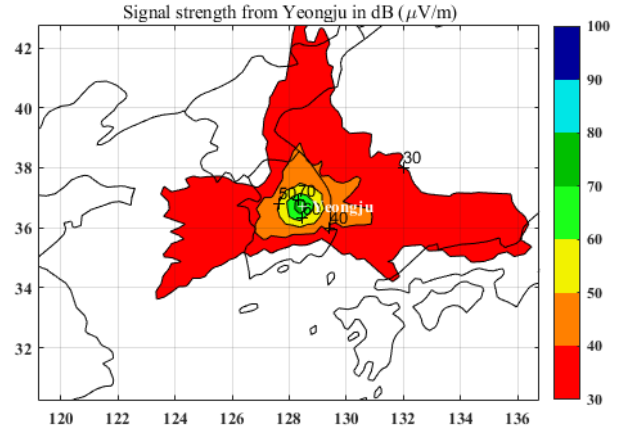


Fig. 2. MF R-Mode signal strength simulation result for the Yeongju transmitter.

conductivity of the area. Thus, the signal strength in Fig. 2 does not uniformly decrease from the Yeongju transmitter.

IV. CONCLUSION

In this study, the parameters (i.e., C , e , and ea) of the approximate signal strength calculation formula for the MF R-Mode system were determined and applied to the simulation tool. The parameters that minimize the least squares error between the results from the GRWAVE and approximate formula were selected. As a case study, the signal strength of the MF R-Mode transmitter in Yeongju was simulated over Korea using the proposed parameters.

ACKNOWLEDGMENT

This research was conducted as a part of the project titled “Development of integrated R-Mode navigation system [PMS4440]” funded by the Ministry of Oceans and Fisheries, Republic of Korea (20200450).

REFERENCES

- [1] P. Misra and P. Enge, *Global Positioning System: Signals, Measurements, and Performance*. Ganga-Jamuna Press, 2011.
- [2] K. Park and J. Seo, “Single-antenna-based GPS antijamming method exploiting polarization diversity,” *IEEE Trans. Aerosp. Electron. Syst.*, vol. 57, no. 2, pp. 919–934, Apr. 2021.
- [3] K. Park, D. Lee, and J. Seo, “Dual-polarized GPS antenna array algorithm to adaptively mitigate a large number of interference signals,” *Aerosp. Sci. Technol.*, vol. 78, pp. 387–396, Jul. 2018.

- [4] S. Kim, K. Park, and J. Seo, "Mitigation of GPS chirp jammer using a transversal FIR filter and LMS algorithm," in *Proc. ITC-CSCC*, 2019.
- [5] E. Schmidt, N. Gatsis, and D. Akopian, "A GPS spoofing detection and classification correlator-based technique using the LASSO," *IEEE Trans. Aerosp. Electron. Syst.*, vol. 56, no. 6, pp. 4224–4237, Dec. 2020.
- [6] K. Park, D. Lee, and J. Seo, "Adaptive signal processing method using a single-element dual-polarized antenna for GNSS interference mitigation," in *Proc. ION GNSS+*, 2017, pp. 3888–3897.
- [7] Y. Jiao and Y. T. Morton, "Comparison of the effect of high-latitude and equatorial ionospheric scintillation on GPS signals during the maximum of solar cycle 24," *Radio Sci.*, vol. 50, no. 9, pp. 886–903, 2015.
- [8] J. Lee, Y. Morton, J. Lee, H.-S. Moon, and J. Seo, "Monitoring and mitigation of ionospheric anomalies for GNSS-based safety critical systems," *IEEE Signal Process. Mag.*, vol. 34, no. 5, pp. 96–110, Sep. 2017.
- [9] J. Seo, T. Walter, and P. Enge, "Availability impact on GPS aviation due to strong ionospheric scintillation," *IEEE Trans. Aerosp. Electron. Syst.*, vol. 47, no. 3, pp. 1963–1973, Jul. 2011.
- [10] H. Lee, S. Pullen, J. Lee, B. Park, M. Yoon, and J. Seo, "Optimal parameter inflation to enhance the availability of single-frequency GBAS for intelligent air transportation," *IEEE Trans. Intell. Transp. Syst.*, 2022, early access.
- [11] A. K. Sun, H. Chang, S. Pullen, H. Kil, J. Seo, Y. J. Morton, and J. Lee, "Markov chain-based stochastic modeling of deep signal fading: Availability assessment of dual-frequency GNSS-based aviation under ionospheric scintillation," *Space Weather*, vol. 19, no. 9, pp. 1–19, Sep. 2021.
- [12] K. Sun, H. Chang, J. Lee, J. Seo, Y. Jade Morton, and S. Pullen, "Performance benefit from dual-frequency GNSS-based aviation applications under ionospheric scintillation: A new approach to fading process modeling," in *Proc. ION ITM*, 2020, pp. 889–899.
- [13] N. Ahmed and J. Seo, "Statistical evaluation of the multi-frequency GPS ionospheric scintillation observation data," in *Proc. ICCAS*, 2017, pp. 1792–1797.
- [14] W. Kim, P.-W. Son, S. G. Park, S. H. Park, and J. Seo, "First demonstration of the Korean eLoran accuracy in a narrow waterway using improved ASF maps," *IEEE Trans. Aerosp. Electron. Syst.*, vol. 58, no. 2, pp. 1492–1496, Apr. 2022.
- [15] P.-W. Son, J. Rhee, Y. Han, K. Seo, and J. Seo, "Preliminary study of multichain-based Loran positioning accuracy for a dynamic user in South Korea," in *Proc. IEEE/ION PLANS*, 2018, pp. 1034–1038.
- [16] P.-W. Son, Y. Han, K. Seo, and T. H. Fang, "Analysis of range measurement based on MF DGNSS infrastructures," *Journal of Positioning, Navigation, and Timing*, 2022, in press.
- [17] Y. Han, S. Park, G. Seol, T. Kim, and T. Hwang, "R-Mode positioning system demonstration," in *Proc. IPNT*, 2021.
- [18] S. Jeong and P.-W. Son, "Preliminary analysis of skywave effects on MF DGNSS R-Mode signals during daytime and nighttime," in *Proc. IEEE ICCE-Asia*, 2022.
- [19] S. Lee, E. Kim, and J. Seo, "SFOL DME pulse shaping through digital predistortion for high-accuracy DME," *IEEE Trans. Aerosp. Electron. Syst.*, vol. 58, no. 3, pp. 2616–2620, June 2022.
- [20] K. Park, W. Kim, and J. Seo, "Effects of initial attitude estimation errors on loosely coupled smartphone GPS/IMU integration system," in *Proc. ICCAS*, 2020, pp. 800–803.
- [21] H. Lee, A. Abdallah, J. Park, J. Seo, and Z. Kassas, "Neural network-based ranging with LTE channel impulse response for localization in indoor environments," in *Proc. ICCAS*, 2020, pp. 939–944.
- [22] H. Lee, J. Seo, and Z. Kassas, "Integrity-based path planning strategy for urban autonomous vehicular navigation using GPS and cellular signals," in *Proc. ION GNSS+*, 2020, pp. 2347–2357.
- [23] S. Jeong, H. Lee, T. Kang, and J. Seo, "RSS-based LTE base station localization using single receiver in environment with unknown path-loss exponent," in *Proc. ICTC*, 2020, pp. 958–961.
- [24] T. Kang and J. Seo, "Practical simplified indoor multiwall path-loss model," in *Proc. ICCAS*, 2020, pp. 774–777.
- [25] T. Kang and Y. Shin, "Indoor navigation algorithm based on a smartphone inertial measurement unit and map matching," in *Proc. ICTC*, 2021, pp. 1421–1424.
- [26] J. Park, S. Jang, and Y. Shin, "Indoor path planning for an unmanned aerial vehicle via curriculum learning," in *Proc. ICCAS*, 2021, pp. 529–533.
- [27] H. Lee, T. Kang, S. Jeong, and J. Seo, "Evaluation of RF fingerprinting-aided RSS-based target localization for emergency response," in *Proc. IEEE VTC*, June 2022.
- [28] H. Lee, J. Seo, and Z. Kassas, "Urban road safety prediction: A satellite navigation perspective," *IEEE Intell. Transp. Syst. Mag.*, 2022, early access.
- [29] M. Jia, H. Lee, J. Khalife, Z. M. Kassas, and J. Seo, "Ground vehicle navigation integrity monitoring for multi-constellation GNSS fused with cellular signals of opportunity," in *Proc. IEEE ITSC*, 2021, pp. 3978–3983.
- [30] S. Kim, H. Lee, and K. Park, "GPS multipath detection based on carrier-to-noise-density ratio measurements from a dual-polarized antenna," in *Proc. ICCAS*, 2021, pp. 1099–1103.
- [31] H. Lee and J. Seo, "A preliminary study of machine-learning-based ranging with LTE channel impulse response in multipath environment," in *Proc. IEEE ICCE-Asia*, 2020.
- [32] H. Lee, T. Kang, and J. Seo, "Development of confidence bound visualization tool for LTE-based UAV surveillance in urban areas," in *Proc. ICCAS*, 2019, pp. 1187–1191.
- [33] T. Kang, H. Lee, and J. Seo, "Analysis of the maximum correlation peak value and RSRQ in LTE signals according to frequency bands and sampling frequencies," in *Proc. ICCAS*, 2019, pp. 1182–1186.
- [34] J. Kim, J.-W. Kwon, and J. Seo, "Simulation study on a method to localize four mobile robots based on triangular formation," in *Proc. ION Pacific PNT*, 2017, pp. 348–361.
- [35] P.-W. Son, J. Rhee, J. Hwang, and J. Seo, "Universal kriging for Loran ASF map generation," *IEEE Trans. Aerosp. Electron. Syst.*, vol. 55, no. 4, pp. 1828–1842, Oct. 2019.
- [36] P. Williams and C. Hargreaves, "UK eLoran—initial operational capability at the port of Dover," in *Proc. ION ITM*, 2013, pp. 392–402.
- [37] W. J. Pelgrum, "New potential of low-frequency radio navigation in the 21st century," Ph.D. dissertation, Delft University of Technology, The Netherlands, Nov. 2006.
- [38] Y. Li, Y. Hua, B. Yan, and W. Guo, "Research on the eLoran differential timing method," *Sensors*, vol. 20, no. 22, p. 6518, 2020.
- [39] W. Kim, P.-W. Son, J. Rhee, and J. Seo, "Development of record and management software for GPS/Loran measurements," in *Proc. ICCAS*, 2020, pp. 796–799.
- [40] J. Park, P.-W. Son, W. Kim, J. Rhee, and J. Seo, "Effect of outlier removal from temporal ASF corrections on multichain Loran positioning accuracy," in *Proc. ICCAS*, 2020, pp. 824–826.
- [41] J. Hwang, P.-W. Son, and J. Seo, "TDOA-based ASF map generation to increase Loran positioning accuracy in Korea," in *Proc. IEEE ICCE-Asia*, 2018.
- [42] G. Johnson, K. Dykstra, S. Ordell, and P. Swaszek, "R-Mode positioning system demonstration," in *Proc. ION GNSS*, 2020, pp. 839–855.
- [43] G. Johnson, P. Swaszek, J. Alberding, M. Hoppe, and J.-H. Oltmann, "The feasibility of R-Mode to meet resilient PNT requirements for e-Navigation," in *Proc. ION GNSS*, 2014, pp. 3076–3100.
- [44] G. Johnson and P. Swaszek, "Feasibility study of R-Mode using MF DGPS transmissions," German Federal Waterways and Shipping Administration, Final Report, Tech. Rep., 2014.
- [45] —, "Feasibility study of R-Mode combining MF DGNSS, AIS, and eLoran transmissions," German Federal Waterways and Shipping Administration, Final Report, Tech. Rep., 2014.
- [46] —, "Feasibility study of R-Mode using AIS transmissions: Investigation of possible methods to implement a precise GNSS independent timing signal for AIS transmissions," German Federal Waterways and Shipping Administration, Final Report, Tech. Rep., 2014.
- [47] G. W. Johnson, P. F. Swaszek, M. Hoppe, A. Grant, and Šafář, "Initial results of MF-DGNSS R-Mode as an alternative position navigation and timing service," in *Proc. ION ITM*, 2017, pp. 1206–1226.
- [48] J. H. Rhee, S. Kim, P.-W. Son, and J. Seo, "Enhanced accuracy simulator for a future Korean nationwide eLoran system," *IEEE Access*, vol. 9, pp. 115 042–115 052, Aug. 2021.
- [49] S. C. Lo, B. B. Peterson, C. O. L. Boyce Jr., and P. K. Enge, "Loran coverage availability simulation tool," in *Proc. ION GNSS*, Sep. 2008, pp. 2595–2605.
- [50] S. Jeong and P.-W. Son, "Development of an R-Mode simulator using MF DGNSS signals," in *Proc. ICCAS*, 2021, pp. 1104–1108.
- [51] M. C. García. (2009, Feb.) Calculation of radio electrical coverage in medium-wave frequencies. Accessed: Aug. 24, 2022. [Online]. Available: http://repositori.uvic.cat/bitstream/handle/10854/252/trealu_a2009_crego_marcos_calculation.pdf?sequence=1&isAllowed=y